FORMATION AND PROPERTIES OF MAGNETITE NANOPARTICLES BY SOL–GEL METHOD

Dr. KANNAN NITHIN K V

Associate Professor,
Department of Physics, Kathir College of Engineering,
Coimbatore, Tamilnadu, India.

Abstract: **Nanoparticles of Magnetite Fe_3O_4 can be synthesized by Ethylene glycol ($C_2H_6O_2$) and Ferric nitrate ($(Fe(NO_3)_3.9H_2O)$) as precursors in Sol-gel method by changing annealing temperatures. The obtained Fe_3O_4nanoparticles are characterized by X-Ray diffraction (XRD), Field Emission Scanning Electron Microscope (FESEM), X-ray energy dispersive spectrometer (EDS) and Vibrating Sample Magnetometer (VSM). From the results, due to change in temperature the size of nanoparticles, saturation magnetization value and covercivity value of nanoparticles are changing. In this method size, covercivity value and saturation magnetization values are increasing with temperature. Under different atmospheres and temperatures the phase transformation of nanoparticles has been studied.**

Keywords: **Sol-Gel Method, Magnetite Nanoparticles Size; Magnetic properties**

1. INTRODUCTION

Nanoparticles are focused of researcher for a wide application, not only because of their properties, but also due to nano size compared with their bulk matching part. Nanoparticles are intermediate between atomic and bulk level. The properties deeply changed due to the nano level conversion, as the size of the particle changes outstanding to their large surface to volume ratio. Due to their spacious applications, a lot of research has been carried out for the synthesis of 1-dimensional (1D) nano structured (nanotubes [1], nanorods [2], nanobelts [3], nanorings [4], nanohelics [5], nanowires [6], nanofibres [7], nano sphere [8] nano flowers [9] and nano sheets [10] like structures.

Magnetic nanoparticles are of spread interest to researchers due to their creditable magnetic properties. Magnetic nano particles have a wide applications in magnetic fluids recording [11], catalysis[12], biotechnology/biomedicine [13], material sciences, photo catalysis[14], electrochemical and bioeletrochemical sensing [15], microwave absorption [16], magnetic resonance imaging [MRI] [17], medical diagnosis, data storage [18], environmental remediation [19] and, as an electrode, for supercapictors and lithium ion batteries (LIB) [20]. While talking of, various magnetic nano particles, magnetite (Fe3O4) has been used for a several wide number of applications due to its superparamagnetic properties but one property of being sensitive to oxidation and agglomeration, has lemmatized its use. Due to its unique and creative applications in every field of life, researchers are paying attention to developing en-number of methods to synthesize magnetic nanoparticles of different sizes, morphology and compositions.

Fe3O4 exists in nature as the mineral magnetite and it has a cubic inverse spinel structure which formed of a cubic close packed array of oxide ions where all of the Fe^{2+} ions occupy half of the octahedral sites and the Fe^{3+} are split evenly across the remaining octahedral sites and the tetrahedral sites [21]. At room temperature electrons can bound between Fe^{2+} and Fe^{3+} ions in the octahedral sites, depiction magnetite an important part of half-metallic materials [22].

A wide range of chemistry-based processes are routed to synthesize nanosized magnetite particles, including precipitation method [23], sol–gel method [24], emulsion technique [25], hydrothermal preparation [26] and DC thermal arc-plasma method [27]. In different chemical synthesis methods for metal oxides preparation sol–gel practice offers numerous advantages over other processes, with good homogeneity, low cost, and high purity. In sol-gel method magnetic nanoparticles can be prepared by using metalloranic precursors [28]. Tang et al. [29] prepared nanostructured magnetite thin film by sol–gel method with reasonably priced reagent of iron (II) chloride as preparatory materials. Magnetite nanoparticles were obtained at 300°C, however, when the temperature increased to 350°C hematite appeared. Due to this problem its usefulness in applications are restricted. On reaction of ferric nitrate with ethylene glycol are reported for synthesis of iron oxides and mixtures of iron oxides by sol-gel method [30], even though, pure magnetite cannot be obtained.

Fe_3O_4 magnetite nanoparticles are successfully synthesized by sol-gel method combined with annealing under vacuum using nontoxic ferric nitrate and ethylene glycol as starting materials. In a moderately longer temperature range of at least 150 – 450°C magnetite nanoparticles can be obtained. The direction is easily controlled during the reaction processes without considering Fe(II)/Fe(III) molar ratio control and basic condition. The sizes of obtained magnetite nanoparticles can be easily modified by changing annealing temperature. And the magnetic properties of these samples were investigated and correlated to the amount and grain-size of the magnetite nanoparticles are evaluated in our work.

2. EXPERIMENTAL

2.1. Materials

From Triveni Chemicals the Ferric nitrate ($Fe(NO_3)_3$ - $9H_2O$) and ethylene glycol ($C_2H_6O_2$) of analytical grade were obtained. The reagents were used without further purification.

2.2. Preparation and characterization nanoparticles

The synthesizing process of magnetite nanoparticles is show in Figure 1, and 0.3 mol ferric nitrates was dissolved in 100ml ethylene glycol solution and stirring vigorous for 3 hour at room temperature, and the solution was heated to 80^{o}C and cooled to get gel. The colour of the gel was brown. After 2 hour the gel dried at 100^{o}C for about 5 hour and then the dried gel was annealed in the temperature range 150^{o}C to 450^{o}C under vacuum. The different size of magnetite nanoparticles was synthesized.

$$Fe(No_3)_3 + HOCH_2CH_2OH \xrightarrow{30^{O}C} Sol \xrightarrow{80^{O}C} Gel \xrightarrow{100^{O}C} Xerogel \xrightarrow{Annealed} Fe_3O_4$$

Fig. 1. Schematic preparation of magnetite nanoparticles

The phase structures of magnetite nanoparticles were carried out by X-ray diffratometer (XRD) Philips PW 3710 with Kα radiation. The XRD study is performed on magnetite nanoparticles specimen over 2θ values of 0 - 80^{o}. The crystalline phases are identified by comparing the peak positions and intensities with data files (JCPDS). The morphologies, sizes and composition analysis of magnetite nanoparticles were obtained using a field emission scanning electron microscopy (FESEM JSM-6700F) equipped with an X-ray energy-dispersive spectrometer (EDS). The magnetization loops for magnetite nanoparticles were measured at room temperature using a vibrating sample magnetometer (VSM, JDM-13).

3. RESULTS AND DISCUSSION

3.1. Characterization of magnetite nanoparticles

The XRD patterns of magnetite nanoparticles obtained at different temperatures are shown in figure 2. The diffraction peaks at 2θ = 34.23^{o}, 57.15^{o}, 29.49^{o}, 53.12^{o} and 37.02^{o} can be assigned to (3 1 1), (4 4 0), (2 2 0), (5 1 1) and (4 0 0) planes of Fe_3O_4 (JCPDS #19-629), respectively. The other diffraction peaks are not corresponding to ferrite nitrite and other oxides. Some diffraction peaks are due to α-Fe_2O_3 and γ-Fe_2O_3 can be observed, but those of Fe_3O_4. This result indicates the purity Fe_3O_4 of resultant nanoparticles. The rising annealing temperature leads to decreases the full-width at half-maximum of the reflection peaks and the reflection peaks become sharper. These indicate that with increasing annealing temperature in the temperature range leads to sizes of nanoparticles increase and the improvement of crystallinity of nanoparticles. Using Scherrer's formula, particle size calculated from XRD peak broadening, is plotted as a function of annealing temperature (Figure 3). From the plot, the Fe_3O_4 nanoparticle size increases from 150 to 450^{o}C, particle size of the Fe_3O_4 nanoparticles synthesized at different temperatures calculated by Scherrer's equations [31]. And the mean particle size are from figure 2 are 9.8 (d), 12.2 (c), 15.3 (b), and 16.4 nm (a) for the temperature range from 150, 250, 350, and 450^{o}C, respectively.

The FESEM micrographs of Fe_3O_4 nanoparticles obtained under vacuum at different temperature are shown in figure 4, and the EDS image of Fe_3O_4 nanoparticles (Figure 5). The 20 nm and 40 nm mean sizes of Fe_3O_4 nanoparticles from figure 4 (a) and (b) were determined for the temperature 150^{o}C and 450^{o}C, respectively. Figure 5 represent the EDS image of as-synthesized Fe_3O_4 nanoparticles. From Figure 5, nanoparticles consist of Fe and O elements, further confirming the appearance of Fe_3O_4 nanoparticles.

3.2. Phase transformation of magnetite nanoparticles

The treatment of different temperatures and atmospheres of synthesized Fe_3O_4 nanoparticles can be transformed easily into α-Fe_2O_3 or α-Fe and γ-Fe_2O_3. Due to higher temperature Fe_3O_4 nanoparticles can be oxidized to γ-Fe_2O_3, which can be further transformed into α-Fe_2O_3 [32].

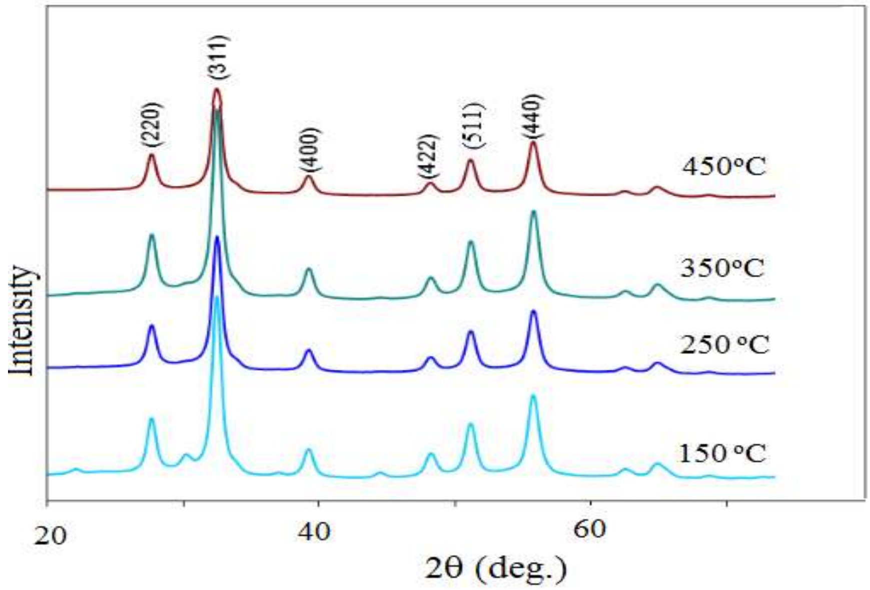

Fig. 2. XRD patterns of magnetite nanoparticles for 3 hour.

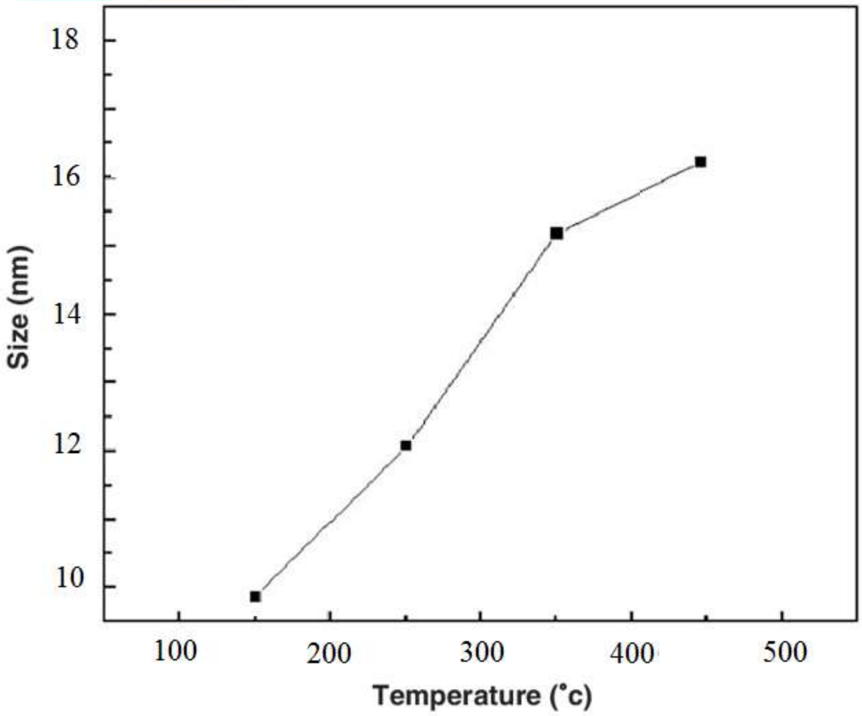

Fig. 3. Magnetite nanoparticles size calculated from XRD peak

Black colour of nanoparticles changes to red brown when it is treated at 300^{o}C in air, due to oxidation. Figure 5 shows that all XRD patent of nanoparticles at different temperature. The peaks of red-brown material match with γ-Fe_2O_3 (JCPDS 39-1346). The results indicate that high-angle peaks are slightly increased to higher angles due to the oxidation of Fe_3O_4 in air, compared with vacuum. From result the oxidation of Fe_3O_4 in air at 300^{o}C leads to γ-Fe_2O_3. Similarly for higher temperature transformations of Fe_3O_4 to γ-Fe_2O_3 are reported [33].

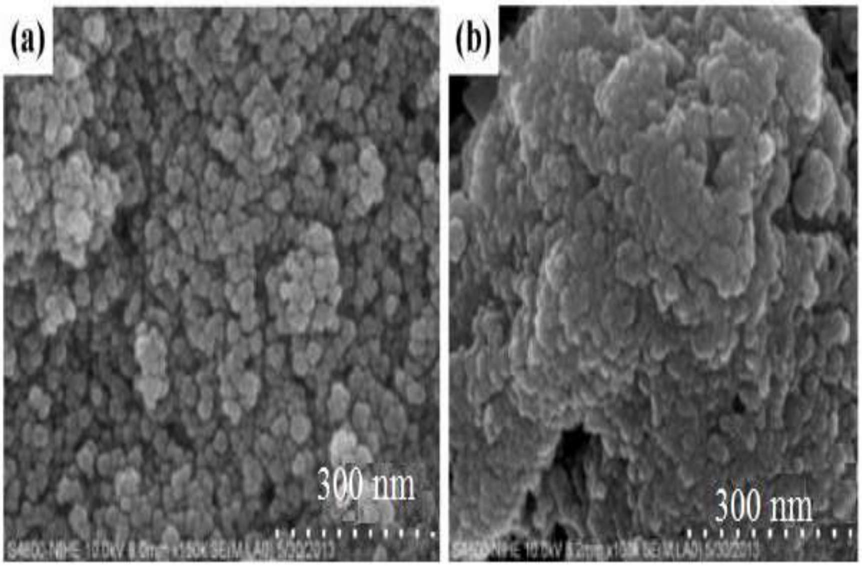

Fig. 4. FESEM pattern of xerogel at (a) 150 ^{o}C and (b) 450^{o}C

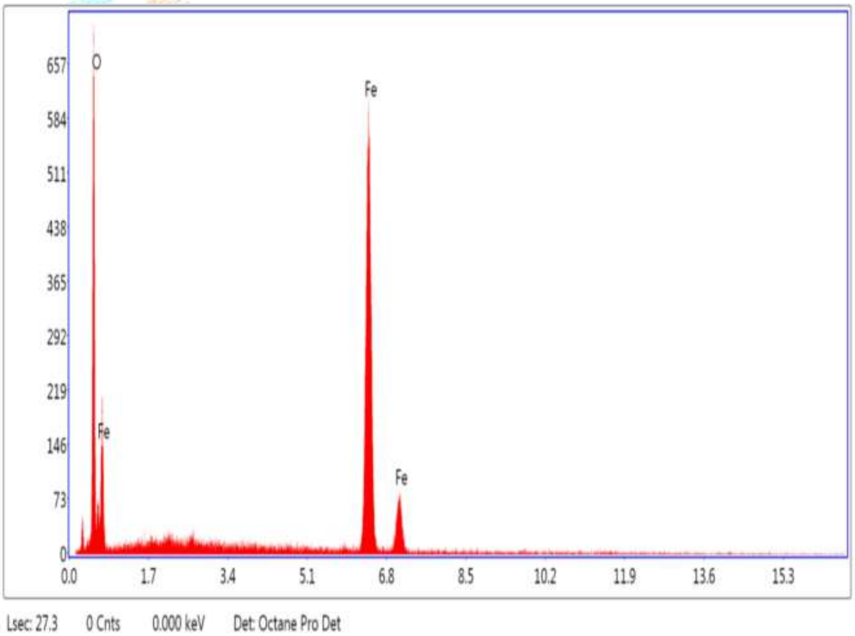

Fig. 5. EDS image of magnetite.

The Fe_3O_4 nanoparticles were reduced to α-Fe after annealing under Ar+5% H_2 at 400^{o}C [34]. From the above results H_2 might be the important factor for the transformation of Fe_3O_4 to α-Fe at a certain temperature.

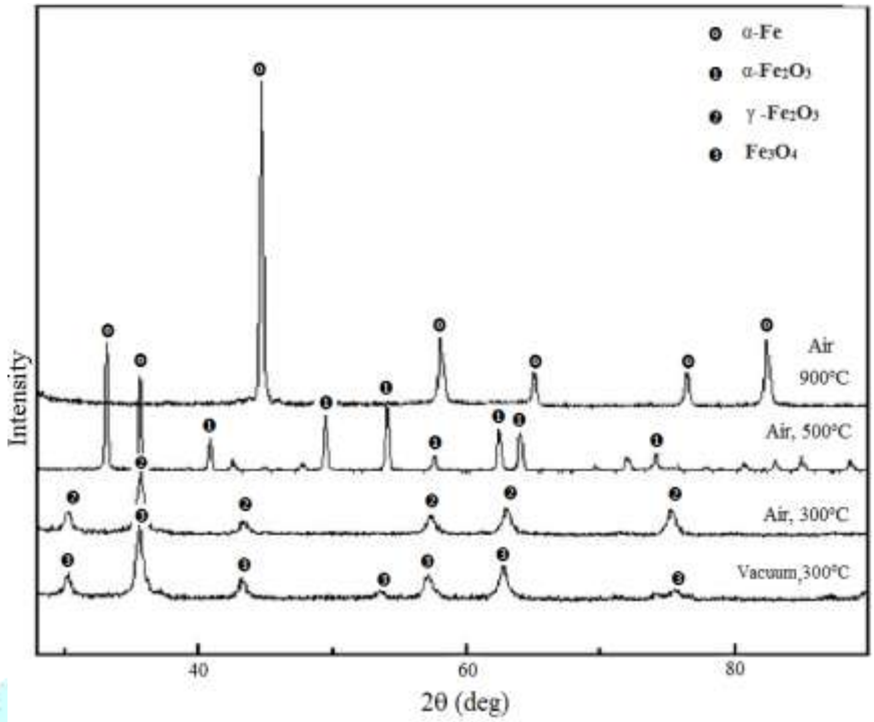

Fig. 5. XRD patterns of Fe_3O_4 nanoparticles at different temperature and atmosphere

In this study, XRD results confirmed (Figure 5); under annealing process the synthesized Fe_3O_4 is reduced to α-Fe (JCPDS 33-0664) in vacuum at 900°C. As the starting material of an organic reagent (ethylene glycol) and the closed system for annealing process, synthesized Fe_3O_4 nanoparticles have a chance to absorb some reductive materials of organic residual materials on their surfaces [34], and due to the absorbed organic residual materials on their surfaces, the synthesized Fe_3O_4 nanoparticles are reduced into α-Fe at 900°C.

3.3. Magnetic behavior of magnetite nanoparticles

Figure 6 shows the magnetic hysteresis loops for Fe_3O_4 nanoparticles measured at room temperature are illustrated. Saturated magnetization (Ms) of Fe_3O_4 nanoparticles obtained at 150, 250, 350, and 450°C are found to be 45, 57, 64and 70 emu/g, respectively. It is known that for increasing annealing temperature in the temperature range studied, the saturated magnetization value increases continuously. In magnetism the particle sizes leads to magnetic behavior of Fe_3O_4 nanoparticles [35]. Saturated magnetization values are increased due to the increase in Fe_3O_4 nanoparticle sizes with increase in annealing temperature. From figure 6 coercivity values Hc are found to be 0.03, 0.06, 0.08 and 0.23 kOe of Fe_3O_4 nanoparticles for different temperature. Due to present of iron oxide particles of 10 nm, superparamagnetic behavior is often observed at room temperature [36]. Even at 150°C 470 nm size of Fe_3O_4 nanoparticles are obtained, superparamagnetic characteristics at room temperature not observed. Due to increasing in annealing temperature the coercivity value of Fe_3O_4 nanoparticles increases for temperature range studied, which can be attributed to the increasing sizes of Fe_3O_4 nanoparticles. Similarly from results the increasing coercivity values with increase in Fe_3O_4 nanoparticles sizes [27].

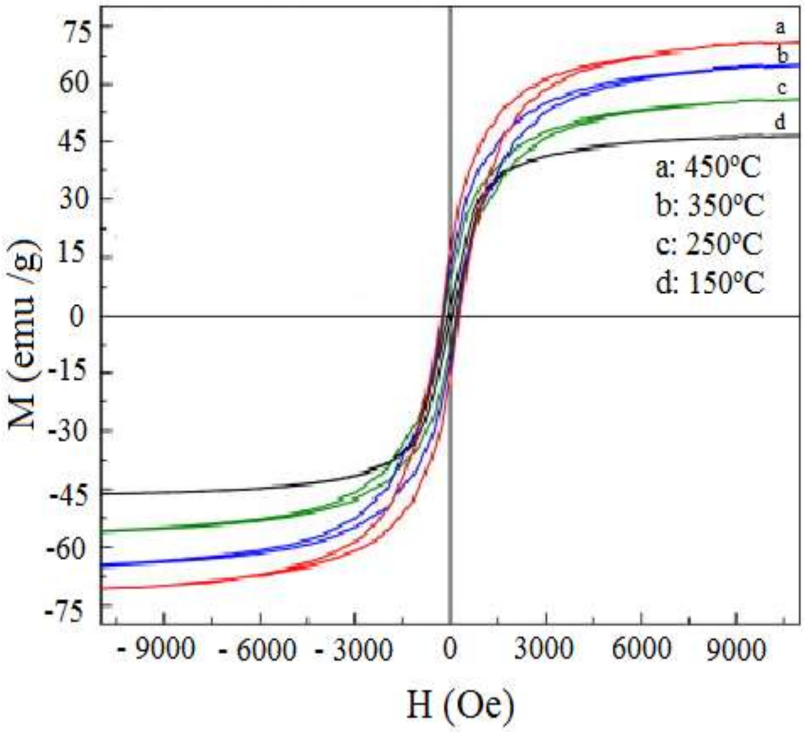

Fig. 6. Magnetization loops of magnetite nanoparticles

4. CONCLUSION

In summary, Samples were prepared by sol–gel method combined with annealing under vacuum for different temperature and Magnetic properties were investigated. From XRD and FESEM results that confirm different size of Fe_3O_4 nanoparticles can be obtained by changing the annealing temperature. Because of increasing Fe_3O_4 particle sizes the saturated magnetization values and coercivity values increase. The synthesized Fe_3O_4 nanoparticles can be easily deformed into γ-Fe_2O_3, α-Fe_2O_3 by treating in air, or α-Fe in vacuum by annealing. The method in this study offers several features for preparation Fe_3O_4 nanoparticles. In this method by change the annealing temperature size can be easily controlled to produce Fe_3O_4 nanoparticles.

REFERENCES

[1] Wen, Z., et al., Silicon nanotube anode for lithium-ion batteries. Electrochemistry Communications, (2013). 29: p. 67-70.

[2] Yang, Z., et al., Facile synthesis of CuO nanorod for lithium storage application. Materials Letters, (2013). 90: p. 4-7.

[3] Mondal, A.K., et al., Highly Porous $NiCo_2O_4$ Nanoflakes and Nanobelts as Anode Materials for Lithium-Ion Batteries with Excellent Rate Capability. ACS applied materials & interfaces, (2014). 6(17): p. 14827-14835.

[4] Nagaraju, G., Ultra long single crystalline Na0. 3V2O5 nanofibers/nanorings synthesized by a facile one pot green approach and their lithium storage behavior. Journal of the Brazilian Chemical Society, (2013). 24(10): p. 1662-1668.

[5] Cui, R., Z. Han, and J.J. Zhu, Helical carbon nanotubes: intrinsic peroxidase catalytic activity and its application for biocatalysis and biosensing. Chemistry-A European Journal, (2011). 17(34): p. 9377-9384.

[6] Wang, X., et al., Revealing the conversion mechanism of CuO nanowires during lithiation–delithiation by in situ transmission electron microscopy. Chem. Commun., (2012). 48(40): p. 4812-4814.

[7] Qie, L., et al., Nitrogen-Doped Porous Carbon Nanofiber Webs as Anodes for Lithium Ion Batteries with a Superhigh Capacity and Rate Capability. Advanced Materials, (2012). 24(15): p. 2047-2050.

[8] Schladt, T.D., et al., Au@ MnO nanoflowers: hybrid nanocomposites for selective dual functionalization and imaging. Angewandte Chemie International Edition, (2010). 49(23): p. 3976-3980.

[9] Pawar, R., et al., Growth of ZnO nanodisk, nanospindles and nanoflowers for gas sensor: pH dependency. Current Applied Physics, (2012). 12(3): p. 778-783.

[10] Zhang, X., et al., Enhanced photoresponsive ultrathin graphitic-phase C3N4 nanosheets for bioimaging. Journal of the American Chemical Society, (2012). 135(1): p. 18-21.

[11] Singamaneni, S., et al., Magnetic nanoparticles: recent advances in synthesis, self-assembly and applications. Journal of Materials Chemistry, (2011). 21(42): p. 16819-16845.

[12] Gao, J., et al., Multifunctional magnetic nanoparticles: design, synthesis, and biomedical applications. Accounts of chemical research, (2009). 42(8): p. 1097-1107.

[13] Xie, T., et al., Synthesis and properties of composite magnetic material $SrCo_xFe_{12-x}O_{19(x=0\sim0.3)}$. Powder Technology, (2012).

[14] An, T., et al., Synthesis of Carbon Nanotube–Anatase TiO_2 Sub-micrometer-sized Sphere Composite Photocatalyst for Synergistic Degradation of Gaseous Styrene. ACS applied materials & interfaces, (2012). 4(11): p. 5988-5996.

[15] Teymourian, H., et al., Fe_3O_4 magnetic nanoparticles / reduced graphene oxide nanosheets as a novel electrochemical and bioeletrochemical sensing platform. Biosensors and Bioelectronics, (2013).

[16] Zhang, B., et al., Microwave absorption enhancement of Fe_3O_4/polyaniline core/shell hybrid microspheres with controlled shell thickness. Journal of Applied Polymer Science, (2013).

[17] Rashad, M. and I. Ibrahim, Structural, microstructure and magnetic properties of strontium hexaferrite particles synthesised by modified coprecipitation method. Materials Technology: Advanced Performance Materials, (2012). 27(4): p. 308-314.

[18] Frey, N.A., et al., Magnetic nanoparticles: synthesis, functionalization, and applications in bioimaging and magnetic energy storage. Chemical Society Reviews, (2009). 38(9): p. 2532-2542.

[19] Ge, J., et al., Superparamagnetic magnetite colloidal nanocrystal clusters. Angewandte Chemie International Edition, 2007. 46(23): p. 4342-4345.

[20] Yoon, T., et al., Electrostatic Self-Assembly of Fe_3O_4 Nanoparticles on Graphene Oxides for High Capacity Lithium-Ion Battery Anodes. Energies, (2013). 6(9): p. 4830-4840.

[21] R.M. Cornell, U. Schwertmann, The Iron Oxides: Structure, Properties, Reactions, Occurrence and Uses, VCH, New York, 1996, pp. 28–29.

[22] E.J.W. Verwey, Nature 144 (1939) 327.

[23] D. Thapa, et al., Mater. Lett. 58 (2004) 2692.

[24] S.A. Corr, et al., J. Mater. Chem. 14 (2004) 944.

[25] G.B. Biddlecombe, et al., J. Mater. Chem. 11 (2001) 2937.

[26] R. Fan, et al., Mater. Res. Bull. 36 (2001) 497.

[27] C. Balasubramaniam, et al., Mater. Lett. 58 (2004) 3958.

[28] Z.H. Zhou, et al., J. Mater. Chem. 11 (2001) 1704.

[29] N.J. Tang, et al., J. Magn. Magn. Mater. 282 (2004) 92.

[30] G.M. da Costa, et al., J. Solid State Chem. 113 (1994) 405.

[31] J.I. Langford and A.J.C. Wilson, J. Appl. Crystallogr. 11 (1978) 102.

[32] G. Bate, in: D.J. Craik (Ed.), Magnetic Oxides Part 2. Wiley, New York, 1975, pp. 705–707.

[33] S. Sun, et al., J. Am. Chem. Soc. 126 (2004) 273.

[34] J. Xu et al., Mater. Sci. Eng. B 132 (2006) 307.

[35] M.A. Lopez-Quintela and J. Rivas, J. Colloid Interface Sci. 158 (1993) 446.

[36] Y. Ni, et al., Chem. Mater. 14 (2002) 1048.